Supporting Information

Bird et al. 10.1073/pnas.1003719108

SI Text

Supporting Text. ***Data.*** The original data from this work can be found online at the National Oceanic and Atmospheric Administration World Date Center for Paleoclimatology (ftp://ftp.ncdc.noaa.gov/pub/data/paleo/paleolimnology/southamerica/peru/pumacocha2011.txt).

Limnology. Pumacocha's limnological characteristics and local climatic conditions were measured at 4-h intervals between May 29, 2007 and May 11, 2008. Lake-level and surface temperature were measured with a Solinst® Levellogger® deployed in a fixed position 22.25 cm above the lake bottom. Air temperature and barometric pressure at the lake were measured with a land-based Solinst® Barologger®. Depth profiles of lake water temperature, pH, dissolved oxygen, and specific conductivity were measured with a Hydrolab® MiniSond® 4a at 1 m intervals in June 2005, August 2006, and May 2007. Samples for alkalinity and lake water isotopes ($\delta^{18}O_{lw}$, and δD_{lw}) were collected from the coring site between June 2005 and May 2008. Additional samples for $\delta^{18}O_{lw}$ and δD_{lw} were collected monthly between August 2006 and July 2008.

Alkalinity was measured in the field with a Hach® field alkalinity kit by titrating water samples to an end point pH of 4.0 with 1.6 N H_2SO_4. The volume of acid consumed was used to calculate milligrams per liter of HCO_3^-. Lake water $\delta^{18}O$ and δD were measured at the University of Arizona Environmental Isotope Laboratory by CO_2 equilibration with a VG602C Finnigan® Delta S isotope ratio mass spectrometer. The reported precision is 0.1‰ for $\delta^{18}O$ and δD. All values are reported as the per mil (‰) deviation from Vienna standard mean ocean water (VSMOW).

Age control. Supported ^{210}Pb activity was estimated from ^{226}Ra activity measured at each sample depth between 0.00 and 30.70 cm at approximately 1-cm intervals (Table S1). Unsupported ^{210}Pb activity was estimated by subtraction of supported activity from the total activity of each level. Sediment ages were determined using the constant rate of supply model and linear accumulation (1). Eighteen radiocarbon (^{14}C) ages were determined by accelerator mass spectrometry (AMS) on selected charcoal fragments at the University of California, Irvine, W. M. Keck Carbon Cycle Accelerator Mass Spectrometry Laboratory (Table S2). Each sample was cleaned and pretreated following standard protocols at the University of Pittsburgh's Radiocarbon Laboratory (2). All AMS ^{14}C ages were calibrated to years A.D./B.C. with the online program CALIB 5.0 (3). The reported ages are the 2σ median probability age with errors that are one-half of the 2σ age range.

Cesium-137 activities peak between 8.7- and 10.5-cm depth, indicating that sediment within this depth interval was deposited at, or just prior to, approximately A.D. 1963 (Fig. S4). Using the mean depth of this interval, we estimated an average sedimentation rate of 0.21 cm y^{-1}. The 8.7- to 10.5-cm depth interval also contains the A.D. 1963 couplet. Based on the depth of the A.D. 1963 couplet, we calculated an average sedimentation rate of 0.20 cm y^{-1}, which agrees well with the ^{137}Cs-based sedimentation rate. These results strongly suggest that the couplets are annually deposited varves. We therefore rely on linear interpolation between varve ages for age control between 0.0 and 103.5 cm. Varve-based ages have an estimated 1% cumulative error.

Four of the six AMS ^{14}C ages from the upper 105 cm of the Pumacocha record are in agreement with the ^{137}Cs and couplet-based ages, whereas two show age reversals (Fig. 2). These anomalous ages may represent old carbon being washed into the system, contamination of the sample with aquatic matter, or emergent littoral vegetation, which partially received its carbon from the lake water, that was burned and introduced to the sediments. Despite the reversals, the agreement between the balance of AMS ^{14}C ages and the couplet-based ages supports the idea that the couplets are deposited annually (Fig. 2).

Unsupported ^{210}Pb varies about a mean in the uppermost sediments between 0.0 and 8.7 cm. Below 8.7 cm, unsupported ^{210}Pb decreases exponentially (Fig. S4; Table S1). The unsupported ^{210}Pb sediment accumulation rate (0.35 cm y^{-1}) was determined using a linear accumulation model. This rate is higher than that calculated from couplet counts and ^{137}Cs and underestimates the age of the ^{137}Cs peak and A.D. 1963 couplet. Uniform ^{210}Pb activities in surface sediments can result from sediment mixing caused by bioturbation or the coring process (4). However, these mechanisms are ruled out by the fact that the Pumacocha sediments are finely laminated to the sediment–water interface. Instead, we suggest that there exists a mobile ^{210}Pb fraction at the colloid or dissolved level that is able to migrate through interstitial pore waters until sediment compaction precludes its movement (5). This phenomenon is capable of affecting the ^{210}Pb profile while not influencing ^{137}Cs (5). For these reasons, the ^{210}Pb data were deemed unreliable and excluded from consideration in development of the age model.

Based on the agreement between ^{137}Cs, AMS ^{14}C, and couplet counts, we conclude that the Pumacocha couplets are varves (annually deposited laminae) and rely solely on these ages in the upper 103.5 cm of the Pumacocha record. Below 103.5 cm we use the remaining 12 AMS ^{14}C ages (Fig. S4; Table S2). The final composite age/depth model is based on linear interpolation between varve-based ages and a 4th order polynomial fit to the AMS ^{14}C age/depth data and anchored to the varve chronology (Fig. S4).

Carbonate sampling and measurement. All samples for $\delta^{13}C$ and $\delta^{18}O$ analysis were soaked in 7% H_2O_2 for at least 24 h and sieved at 63 µm. The <63-µm fraction was soaked in a 50% bleach solution for 6 to 8 h, rinsed three times with deionized water, vacuum freeze dried, and homogenized. Carbonate isotope samples were measured at the University of Pittsburgh using a GV Instruments, Ltd. (now Isoprime, Ltd., a subsidiary of Elementar Analysensysteme) Isoprime™ stable isotope ratio mass spectrometer and Multi-Prep™ inlet module and Gilson autosampler. Stable isotope measurements were also completed at the University of Arizona using an automated carbonate preparation device (Thermo Finnigan KIEL-III) coupled to a gas-ratio mass spectrometer (Finnigan MAT 252). Powdered samples were reacted with dehydrated phosphoric acid under vacuum at 70 °C (Arizona) and 90 °C (Pittsburgh). Results are reported in conventional delta notation as the per mil (‰) deviation from Vienna Pee Dee Belemnite (VPDB). Results were calibrated to the standards NBS-19 and NBS-18. Precision is ±0.1‰ for $\delta^{18}O_{cal}$ $\delta^{13}C$ (1σ). Replicate sample measurements yielded an internal sample reproducibility of ±0.02‰ for $\delta^{18}O_{cal}$ and ±0.03‰ for $\delta^{13}C_{cal}$.

Conversion of $\delta^{18}O_{cal}$ (VPDB) to $\delta^{18}O_{lw}$ (VSMOW). Authigenic carbonate collected within the littoral zone of the Pumacocha basin in August 2006 and May 2008 had measured $\delta^{18}O_{cal}$ values of −12.2‰ and −12.4‰ (VPDB), respectively (Table S4). Sediment trap $\delta^{18}O_{cal}$ collected between August 2006 and May 2007 averaged −12.8‰ and varied by 0.8‰ with a maximum of −12.4‰ and a minimum of −13.2‰. These values were converted to the VSMOW scale using the standard equation:

$$\delta^{18}O_{(VSMOW)} = 1.03091 \times \delta^{18}O_{(VPDB)} + 30.91.$$

The converted calcite $\delta^{18}O$ values were then used to calculate the predicted values of $\delta^{18}O_{lw}$ for the individual years during which the calcite samples were collected with the equation:

$$\delta^{18}O_{H_2O(VSMOW)} = \frac{\delta^{18}O_{cal(VSMOW)} + 10^3}{\alpha_{cal\text{-}H_2O}} - 10^3,$$

where $\alpha_{cal\text{-}H_2O}$ is the temperature-dependent fractionation factor described by the Kim and O'Neil (6) equation:

$$10^3 \ln \alpha_{cal\text{-}H_2O} = \frac{18.03 \times 10^3}{T_K} - 32.42.$$

Solinist and Hydrolab surface temperature data rounded to the nearest 0.5 °C were used to estimate the temperature of calcite formation for littoral and sediment trap calcite (Table S4).

1. Appleby PG, Oldfield F (1978) The calculation of lead-210 dates assuming a constant rate of supply of unsupported lead-210 to the sediment. *Catena* 5:1–8.
2. Abbott MB, Stafford TW (1996) Radiocarbon geochemistry of modern and ancient Arctic lake systems, Baffin Island, Canada. *Quat Res* 45:300–311.
3. Stuiver M, Reimer PJ (1993) Extended ^{14}C database and revised CALIB radiocarbon calibration program. *Radiocarbon* 35:215–230.
4. Appleby PG, Oldfield F (1983) The assessment of ^{210}Pb data from sites with varying sediment accumulation rates. *Hydrobiologia* 103:29–35.
5. Abril JM (2003) Difficulties in interpreting fast mixing in the radiometric dating of sediments using ^{210}Pb and ^{137}Cs. *J Paleolimnol* 30:407–414.
6. Kim S-T, O'Neil JR (1997) Equilibrium and nonequilibrium oxygen isotope effects in synthetic carbonates. *Geochim Cosmochim Acta* 61:3461–3475.

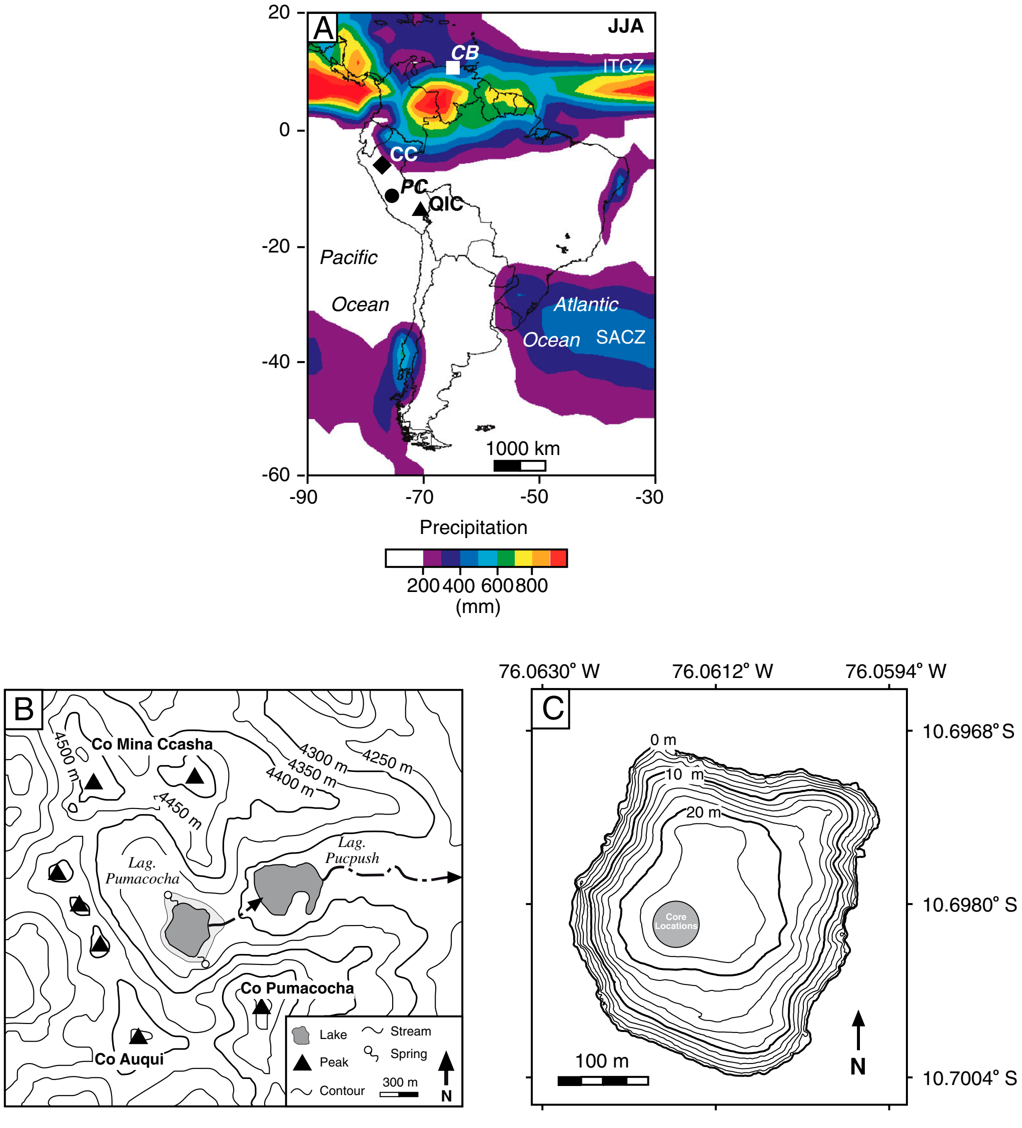

Fig. S1. (*A*) Map of South America showing the locations of records discussed in the text (CB, Cariaco Basin; CC, Cascayunga Cave; PC, Pumacocha; QIC, Quelccaya Ice Cap). Regions with precipitation >200 mm during the austral winter (June–August) are colored. Maxima over the oceans are related to low-level convergence within the Intertropical Convergence Zone (ITCZ) and the South Atlantic Convergence Zone (SACZ). Summer precipitation maxima over South America are associated with the South American summer monsoon. (*B*) Topographic map of the Pumacocha watershed and surrounding region. The gray area fringing the lake indicates the location of wetlands around Pumacocha. (*C*) Bathymetric map of Pumacocha with the coring location marked by a gray circle.

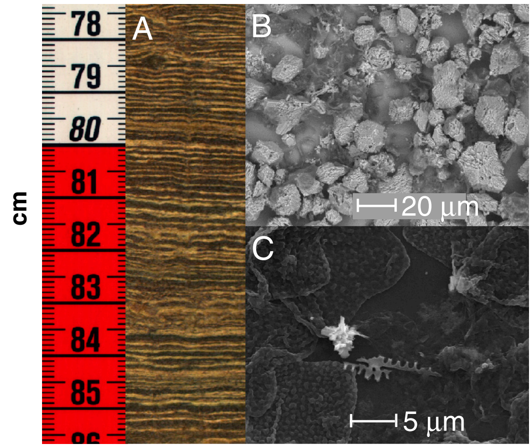

Fig. S2. (*A*) Digital image of sediments from Pumacocha core C-01, drive 1, showing millimeter scale varves representative of those preserved in the upper 176.5 cm of the 579.0-cm Holocene-length sediment record. (*B*) SEM image of the carbonate laminae showing the micron size calcite crystals. (*C*) SEM image of the organic laminae.

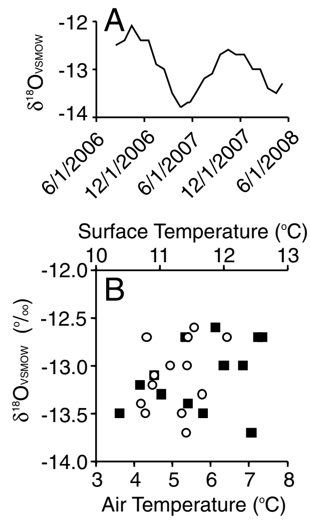

Fig. S3. (*A*) Monthly $\delta^{18}O_{lw}$ (VSMOW) measurements of Pumacocha surface waters plotted versus time show a strong oscillatory signal that tracks the seasonal cycle of precipitation at Pumacocha. (*B*) $\delta^{18}O_{lw}$ (VSMOW) of monthly surface water samples from Pumacocha versus surface air temperatures (circles) and lake surface temperatures (squares).

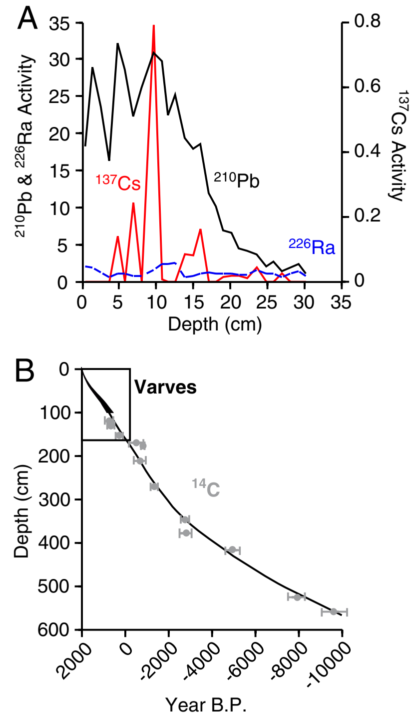

Fig. S4. (*A*) Results of ^{137}Cs, ^{210}Pb and ^{226}Ra analysis. (*B*) Age–depth relationships for the Holocene-length Pumacocha record. AMS ^{14}C ages are shown in gray with error bars. Varve ages are shown in black with the 1% cumulative error. The black line is the 4th order polynomial that was fit to the AMS ^{14}C and anchored to the varve ages.

Table S1. Pumacocha ^{137}Cs, ^{210}Pb, and ^{226}Ra results from freeze core D-08 shown in Fig. S4

Top depth, cm	Bottom depth, cm	Dry BD, g/cm^3	^{210}Pb activity, dpm/g	^{210}Pb 1σ error	^{226}Ra activity, dpm/g	^{226}Ra 1σ error	Excess ^{210}Pb activity, dpm/g	Excess ^{210}Pb activity 1σ error	^{137}Cs activity, dpm/g	^{137}Cs1σ error
0.00	0.85	0.0364	18.328	0.623	1.989	0.672	16.521	0.926	0.000	0.010
0.85	1.75	0.0454	29.019	0.871	1.895	0.816	27.434	1.207	0.000	0.007
1.75	3.10	0.0536	23.525	0.958	1.219	0.988	22.565	1.392	0.000	0.005
3.10	4.20	0.0521	16.231	0.855	0.507	0.660	15.907	1.093	0.000	0.007
4.20	5.30	0.0645	32.196	0.775	1.024	1.306	31.539	1.537	0.139	0.037
5.30	6.25	0.0965	28.543	1.014	1.084	0.339	27.789	1.082	0.000	0.017
6.25	7.45	0.0719	22.291	0.986	0.698	0.930	21.854	1.372	0.244	0.066
7.45	8.70	0.0568	26.211	1.269	0.684	0.990	25.838	1.629	0.000	0.008
8.70	10.50	0.0808	30.815	1.087	1.486	1.379	29.689	1.777	0.790	0.103
10.50	11.05	0.1139	29.697	0.473	2.348	0.135	27.688	0.499	0.005	0.011
11.05	12.10	0.1252	22.434	0.719	2.429	0.151	20.258	0.743	0.000	0.003
12.10	13.10	0.1063	25.177	0.726	2.583	0.909	22.881	1.178	0.000	0.014
13.10	14.45	0.1042	19.369	0.756	0.597	0.179	19.012	0.787	0.082	0.035
14.45	15.45	0.1119	17.914	0.655	0.747	0.723	17.388	0.988	0.080	0.030
15.45	16.50	0.0861	18.642	0.764	1.060	0.760	17.810	1.091	0.161	0.046
16.50	17.50	0.1324	11.980	0.282	1.208	0.418	10.912	0.511	0.000	0.007
17.50	18.50	0.1096	10.103	0.464	1.087	0.392	9.136	0.615	0.000	0.003
18.50	19.70	0.1529	6.955	0.344	1.144	0.573	5.890	0.677	0.013	0.016
19.70	20.50	0.1244	6.560	0.273	1.037	0.203	5.583	0.344	0.017	0.014
20.85	21.70	0.1762	4.442	0.156	0.879	0.562	3.611	0.591	0.018	0.009
21.70	22.90	0.1934	4.178	0.144	0.831	0.072	3.394	0.164	0.011	0.008
22.90	24.30	0.1881	3.699	0.190	1.502	0.139	2.228	0.239	0.043	0.014
24.30	25.35	0.1756	2.072	0.157	0.997	0.130	1.091	0.207	0.000	0.003
25.35	26.40	0.1735	2.619	0.137	1.079	0.312	1.564	0.346	0.000	0.003
26.40	27.50	0.1771	1.419	0.156	0.590	0.329	0.840	0.369	0.026	0.015
27.50	28.75	0.1799	1.845	0.147	1.046	0.171	0.811	0.229	0.000	0.003
28.75	29.75	0.1366	2.368	0.217	1.460	0.124	0.922	0.254	0.000	0.004
29.75	30.70	0.1521	1.128	0.142	0.789	0.365	0.344	0.398	0.000	0.003

Table S2. Radiocarbon ages from Pumacocha

UCI #	Core	Top depth, cm	Bottom depth, cm	Material	Fraction modern	^{14}C age, year B.P.	2-σ median calibrated age range, cal year B.P.	2-σ calibrated median age, cal year B.P.	One-half 2-σ calibrated range (years ±)
32685	A-05	37.5	41.5	charcoal	0.9314	570	578–652	600	35
25283	A-05	49.5	51.5	charcoal	0.9454	450	483–530	510	25
22751	A-05	62	64	charcoal	0.9258	620	551–658	600	55
32683	A-05	72.6	75.6	charcoal	0.9108	750	646–773	690	65
22752	A-05	81.5	82.5	charcoal	0.9267	610	520–673	600	75
22753	A-05	103	105	charcoal	0.8754	1070	929–1016	980	45
22754	A-05	121	123	charcoal	0.8546	1260	1077–1283	1200	105
32682	A-05	129	131	charcoal	0.8420	1380	1220–1390	1300	85
22756	A-05	156	159	charcoal	0.8064	1730	1549–1714	1640	85
32681	A-05	171.7	173.7	charcoal	0.7456	2360	2299–2621	2430	160
25284	A-05	177.7	179.7	charcoal	0.7233	2605	2695–2794	2740	50
32684	A-05	211.5	215.5	charcoal	0.7309	2520	2466–2745	2590	140
25285	A-05	273.9	275.9	charcoal	0.6844	3045	3205–3356	3270	75
25286	A-05	351.3	353.3	charcoal	0.5959	4160	4576–4772	4700	100
25287	A-05	381.3	383.3	charcoal	0.5949	4170	4572–4837	4710	135
43544	E-06	420.7	421.7	charcoal	0.4722	6030	6675–7032	6890	180
43545	E-06	527.3	528.3	charcoal	0.3348	8790	9579–9964	9830	195
43546	E-06	562.3	565.3	charcoal	0.2868	10030	11247–11838	11560	295

Table S3. Equations and statistics for the global meteoric water line (GMWL), local meteoric water line (LMWL). and local evaporation line (LEL)

Line	Equation	r^2	p
GMWL	$\delta D = 7.96 * (\delta^{18}O) + 8.86$*		
LMWL	$\delta D = 7.24 * (\delta^{18}O) - 7.07$	0.90	<0.05
LEL	$\delta D = 5.43 * (\delta^{18}O) - 31.72$	0.89	<0.05
LMWL = LEL	$-13.6‰\ \delta^{18}O$		

Also shown is the $\delta^{18}O$ value where the LEL intersects the LMWL (LMWL = LEL).
*Rozanski et al. (1)

1. Rozanski K, Araguas-Araguas L, Conginatine R (1993) Isotopic patterns in modern global precipitation. *Climate Change in Continental Isotopic Records (Geophysical Monograph)*, eds Swart PK, Lohmann KC, McKenzie J, Savin S (American Geophysical Union, Washington, DC), Vol 78, pp 1–36.

Table S4. Measured oxygen isotope values of calcite from Pumacocha compared with the predicted and measured oxygen isotopic composition of lake water

Sample type	Date collected	Measured $\delta^{18}O_{cal}$ (VPDB)	Predicted $\delta^{18}O_{lw}$ (VSMOW)	Measured $\delta^{18}O_{lw}$ (VSMOW)	Temperature of formation °C	Modeled $\delta^{18}O_{precip}$
Littoral calcite	8/13/2006	−12.2	−12.8	−12.7	11.0	
Sediment trap calcite	8/13/2006 to 5/25/2007	−12.8	−12.9	−12.9	13.0	
Littoral calcite	5/13/2008	−12.4	−13.0	−13.0	11.0	
Average		−12.5	−13.0	−13.0		−12.9

Table S5. Name, type, and length of cores collected from Pumacocha

Core	Core type	Length (cm)	Sediment interface
A-05*	pistion	535	no
B-05	surface	70	yes
C-06*	piston	579	no
D-06	surface	145	yes
E-06	freeze	55	yes
A-07	freeze	62	yes
B-07*	freeze	58	yes
C-07	freeze	60	yes
D-07*	freeze	65	yes
A-08	freeze	69	yes
B-08	freeze	72	yes
C-08	freeze	72	yes
D-08*	freeze	69	yes
E-08	freeze	70	yes
F-08	freeze	74	yes

*Core used in the composite record.